INVOTEK
Jurnal Inovasi Vokasional dan Teknologi
http://invotek.ppj.unp.ac.id/index.php/invotek

Vol. 25, No. 3, Oct 2025
ISSN: 1411 – 3411 (p)
ISSN: 2549 – 9815 (e)

Electronic Load Controller for Induction Generators in Pico-Hydropower Systems: Hardware Analysis and Design

Krismadinata[1,2] *, Ali Basrah Pulungan[1,2]

[1] Department of Electrical Engineering, Faculty of Engineering, Universitas Negeri Padang
Jl. Prof. Dr. Hamka Kampus UNP, Air Tawar Padang, West Sumatra, Indonesia-25131

[2] Professional Engineer Program, Faculty of Engineering, Universitas Negeri Padang
Jl. Prof. Dr. Hamka Kampus UNP, Air Tawar Padang, West Sumatra, Indonesia-25131

*Corresponding author: krismadinata@ft.unp.ac.id Doi: https://doi.org/10.24036/invotek.v25i3.1319

Abstract

Pico-hydropower plants (PHP) utilize water flow energy with low head to generate small-scale electrical power. In induction generator–based PHP systems, changes and imbalance in three-phase loads can disturb voltage and frequency. This study analyzes and develops the hardware design of an electronic load controller (ELC) based on a three-phase AC-AC converter for an induction-generator-based pico-hydropower system. The design process comprised analysis of the system and generator characteristics, specification of hardware requirements, development of the power and control circuits, and integration of the selected components. The proposed ELC directs surplus active power to a dump load, while independently controlled TRIACs enable per-phase power regulation. The resulting design integrates the excitation capacitor, measurement circuits, gate drivers, an arduino mega controller and the AC-AC power stage. It provides a basis for subsequent prototype validation under balanced, varying, and unbalanced loads. Because experimental performance testing was not conducted, its effects on voltage regulation, frequency stability, harmonics, and long-term reliability remain to be established.

Keywords: Self-Excited Induction Generator, Pico Hydropower, Electronic Load Controller, Three-Phase AC-AC Converter.

1. Introduction

Reliable access to electricity remains limited in many remote and rural areas, sustaining interest in small renewable generation systems. Pico-hydropower plants (PHPs) use low-head water flows and relatively small discharges to produce electricity at pico-to micro-scale capacities [1], [2]. Their comparatively simple construction, modest investment requirements, and suitability for off-grid locations make them a practical option where conventional grid extension is difficult.

Induction machines are commonly used as generators in pico-hydropower applications because they are readily available, mechanically robust, and require limited maintenance [3], [4]. However, the use of induction generators in stand-alone power generation systems poses significant challenges for maintaining voltage and frequency stability. This limitation arises from the inherent characteristics of induction generators, whose performance is highly dependent on load conditions. Consequently, variations and fluctuations in the connected load directly affect the output characteristics of the system [5], [6]. The problem becomes more pronounced when consumer loads vary independently across the three phases. Uneven loading can produce voltage fluctuations, frequency deviations, additional losses, and deterioration in delivered power quality [6], [7]. A load controller must therefore maintain the power balance seen by the generator while accommodating both balanced and unbalanced operating conditions.

An electronic load controller (ELC) addresses this requirement by directing surplus generator power to a supplementary resistive load, commonly termed a dump load, so that the total power demand on the generator remains approximately constant [8], [9]. ELCs for microhydro and pico-hydropower

Received date 13/01/2026, Revised date 18/05/2026, Accepted date 23/07/2026

P-ISSN: 1411-3414
E-ISSN: 2549-9815

systems have been implemented with AC-DC-AC and AC-AC converter structures and a variety of control methods [9], [10]. Much of this work emphasizes control algorithms or reports performance through simulation and experimental testing. Comparatively less attention is given to the detailed hardware architecture needed for per-phase regulation under unbalanced three-phase loads.

A practical ELC design consequently requires coordinated decisions regarding converter topology, semiconductor devices, sensing, isolation, protection, and the interface between the power and control circuits [9]–[11]. This study analyzes and develops the hardware design of an ELC based on a three-phase AC-AC converter for an induction-generator-based pico-hydropower system. The design covers generator and system characteristics, the converter power stage, sensing and control circuits, and integration of the main hardware components.

The contribution is a hardware-oriented ELC architecture in which each phase is controlled independently, supported by an excitation-capacitor calculation based on machine data and by isolated sensing and gate-driving circuits. The design is intended as a basis for subsequent prototype testing under varying and unbalanced three-phase loads rather than as evidence of validated system performance.

2. Method

The research methodology employed in this study was systematically designed to support the analysis and hardware design of an electronic load controller (ELC) for an induction generator-based pico-hydropower plant (PHP) system [9], [10]. The procedure comprised four stages: literature review, analysis of hardware requirements, hardware design and assembly, and design finalization. Figure 1 summarizes the sequence of activities.

Figure 1. Research Flowchart

2.1 Literature Review

The first stage reviewed publications on pico-hydropower systems, stand-alone induction generators, ELC principles, power conversion, and load control [8], [9], [12], [13]. The review established the functional requirements of the proposed hardware and provided a basis for comparing converter arrangements reported for small-scale generation. The analysis focused on the design choices used in earlier ELC systems, particularly their converter structures, sensing arrangements, control interfaces, and suitability for small generating units. Their reported advantages and limitations informed the technical specifications adopted for the induction-generator-based pico-hydropower application.

P-ISSN: 1411-3414
E-ISSN: 2549-9815

2.2 Analysis of Hardware Component Requirements

Hardware requirements were then defined from the intended operating conditions of the pico-hydropower system. The analysis considered the induction generator rating, nominal voltage and frequency, and the possibility that three-phase consumer loads would vary and become unbalanced. These requirements guided the specification of the power and control circuits. The power-stage analysis covered the three-phase AC-AC converter, semiconductor switches, protection circuits, and dump load. The control-stage analysis addressed electrical sensors, signal-conditioning and isolation circuits, and the controller used to regulate the diversion of surplus power. Components were selected with reference to the functional, reliability, and safety needs of the integrated system.

2.3 Hardware Design and Assembly

After the requirements had been defined, schematics for the ELC power and control circuits were developed as an integrated design. Component compatibility, power capacity, electrical isolation, and practical assembly were considered throughout this stage. The power circuit used a three-phase AC-AC converter to regulate the power sent to the dump load, while the control circuit generated switching signals in response to the measured operating conditions of the induction generator. The selected components were then arranged and interconnected according to the schematics, producing a hardware configuration for conceptual analysis and subsequent prototype development.

2.4 Design Finalization

The final stage reviewed and refined the completed ELC design. Its conformity with the study objectives and the specified operating conditions of the pico-hydropower system was examined. The review considered whether the power and control circuits were integrated coherently, whether the required load-control functions were represented, and whether the design documentation was sufficiently complete for further implementation. The output of this stage was a documented ELC hardware design intended for later fabrication and testing under varying and unbalanced three-phase loads.

3. Result and Discussion

The design process produced an integrated hardware architecture for a three-phase AC-AC converter-based ELC connected to a stand-alone induction generator. The architecture combines the excitation system, electrical measurements, microcontroller-based processing, isolated gate drivers, and a resistive dump-load power stage.

Load variation and phase imbalance were treated as the main operating conditions that the design must accommodate. Direct AC-AC conversion was selected so that the power absorbed by the dump load could be adjusted without an intermediate DC link or an intentional change to the source frequency. Independent switching channels were assigned to the three phases to support per-phase regulation. The resulting configuration defines the component arrangement and signal paths required for a subsequent ELC prototype. Its expected function is to maintain a more consistent total demand on the generator as consumer loading changes; the actual regulation performance remains subject to experimental validation

3.1 Hardware Design

The proposed ELC regulates generator loading by directing surplus active power to a dump load. Its power stage uses a three-phase AC-AC converter connected to the output of the self-excited induction generator (SEIG). This topology was selected because the delivered power can be adjusted through phase-angle control without converting the AC supply to DC or intentionally changing the fundamental frequency. The SEIG output is sampled by the voltage, current, and frequency measurement circuits and processed by an Arduino Mega microcontroller. Based on these measurements, the controller generates switching commands for the power stage. The TRIACs determine how much surplus power is transferred to the dump load, allowing the total generator loading to be adjusted as consumer demand changes (Figure 2).

P-ISSN: 1411-3414
E-ISSN: 2549-9815

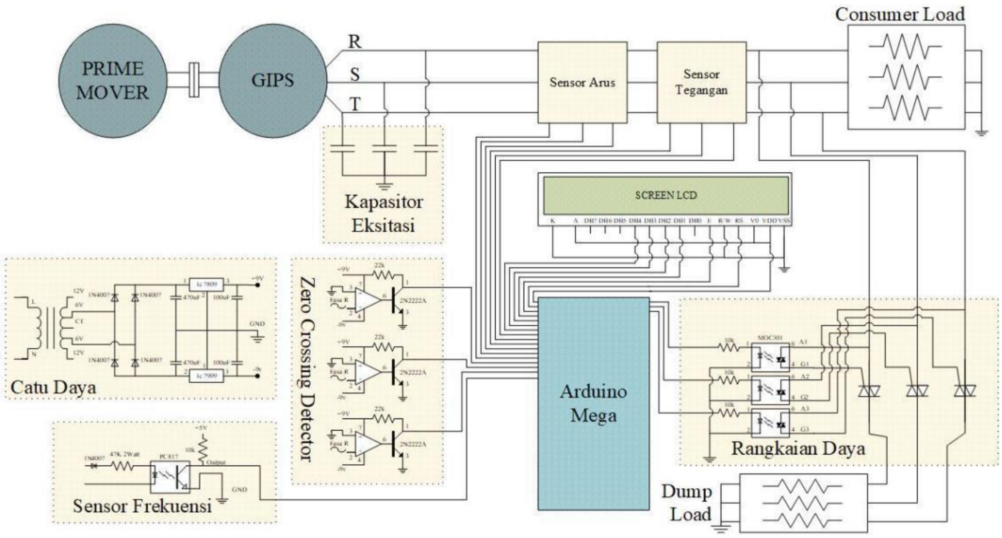

Figure 2. Overall Circuit Configuration of the ELC and SEIG System

3.1.1 Excitation Capacitor Design

A self-excited induction generator (SEIG) requires capacitive reactive power to establish the magnetic flux needed for independent voltage generation. The excitation capacitor supplies this reactive power when no external grid is available. Its value must therefore be matched to the machine and intended operating condition; insufficient or excessive capacitance can prevent stable excitation or shift the generated voltage from the required level (Figure 3).

Figure 3. Nameplate of the Three-Phase Induction Motor

The capacitor design began with the induction motor nameplate data, including rated power, voltage, current, frequency, and power factor. The machine magnetization characteristic was then obtained from the saturation test, which relates the generated voltage and magnetizing current to rotational speed. These data were used in the stated equations to calculate the capacitance required for SEIG operation (Table 1).

Table 1. Three-Phase Induction Motor Nameplate Data

No.	Nameplate Data	Description
1	TYPE Y100L1-4	Manufacturer motor type
2	2.2 kW	Rated power of 2200 W
3	3 HP	Horsepower equivalent to 3 × 745 W
4	50 Hz	Operating frequency
5	220 / 380 V	Rated voltage
6	8.7 / 5.0 A	8.7 A for Δ / 5.0 A for Y

P-ISSN: 1411-3414
E-ISSN: 2549-9815

7	1430 rpm	Motor rotational speed
8	INS CL B	Insulation Class B
9	GU CL IP44	Ingress protection rating
10	DUTY S1	Continuous duty cycle
11	CONN Δ / Y	Delta / Star connection
12	NO. B0 13	Motor serial number
13	34 kg	Motor weight

Table 2 and Figure 4 present the saturation-test measurements obtained from the 2200 W three-phase induction machine.

Tabel 2. Saturation Test Data

No.	Inverter Frequency	Eg (Volt)	Im (Ampere)	n (rpm)
1	0 Hz	0 V	0 A	0 rpm
2	10 Hz	135 V	1.93 A	299 rpm
3	20 Hz	206 V	2.2 A	599 rpm
4	30 Hz	269 V	2.34 A	899 rpm
5	40 Hz	327 V	2.34 A	1198 rpm
6	50 Hz	385 V	2.34 A	1500 rpm

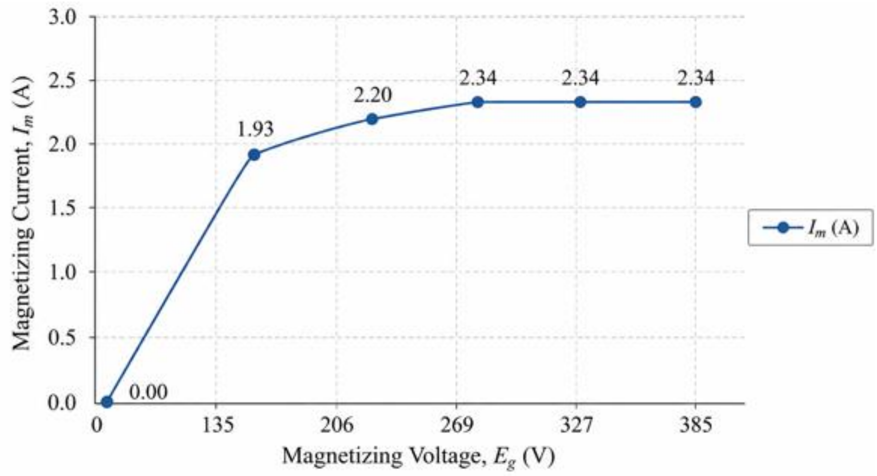

Figure 4. Magnetization Curve

The magnetizing reactance value (X_m) was obtained from the saturation test data at an inverter frequency of 50 Hz using the following equation:

$$X_m = \frac{E_g}{I_m} \quad (1)$$

$$X_m = \frac{385\ V}{2.34\ A} = 164.52\Omega \quad (2)$$

The excitation capacitor value was then determined using the following equations:

$$X_c = X_m = 164.52\ \Omega \quad (3)$$

$$C = \frac{1}{2\pi f X_c} \quad (4)$$

$$C = \frac{1}{2x3.14x50x164.52}$$

$$C = 1.9340008e - 5$$

$$C = 19{,}34\ \mu F$$

3.1.2 Zero Crossing Detector Design

The zero-crossing detector (ZCD) identifies the instants at which the sinusoidal AC voltage passes through zero (Figure 5). These timing points are required for frequency measurement and phase-referenced control of the AC power switches. The circuit uses a 4N25 optoisolator to separate the high-voltage power side from the low-voltage control side, reducing the exposure of the microcontroller circuit to power-system disturbances.

The 230 V AC input is first applied to a parallel resistor network that limits current and is then rectified by a diode bridge. The rectified waveform drives the 4N25 optoisolator, whose transistor output produces a narrow 5 V logic pulse around each zero crossing. This pulse can be read by the microcontroller for timing and frequency calculations.

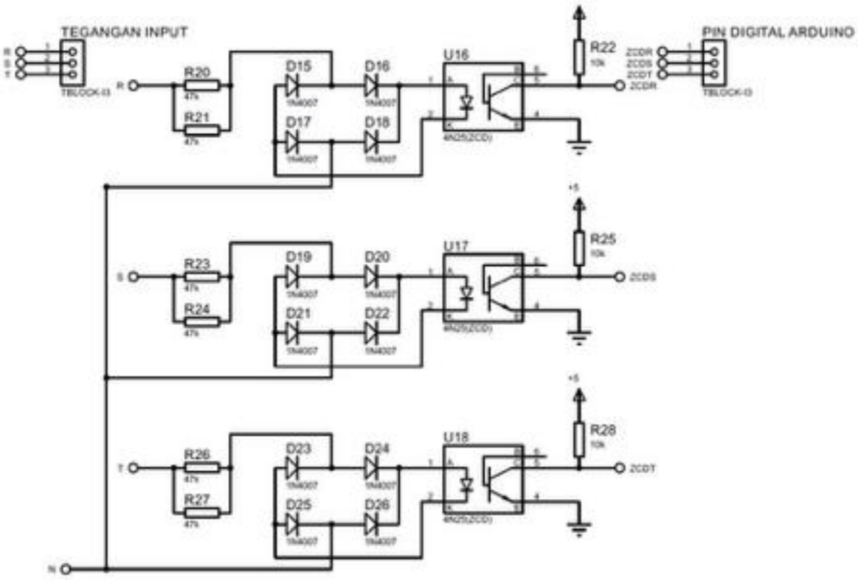

Figure 5. Schematic Diagram of the Zero Crossing Detector Circuit

3.1.3 Frequency Sensor Design

The frequency sensor measures the SEIG output frequency used as feedback by the ELC controller. Because frequency reflects the balance between mechanical input and electrical demand, the measured value is used to identify changes in the generating system's operating condition. The sensor uses a PC817 optoisolator to provide electrical separation between the generator voltage and the control circuit. The SEIG sinusoidal voltage activates the optoisolator, converting successive waveform periods into low-voltage pulses. The arduino mega processes the pulse interval to determine the frequency value supplied to the ELC control routine (Figure 6).

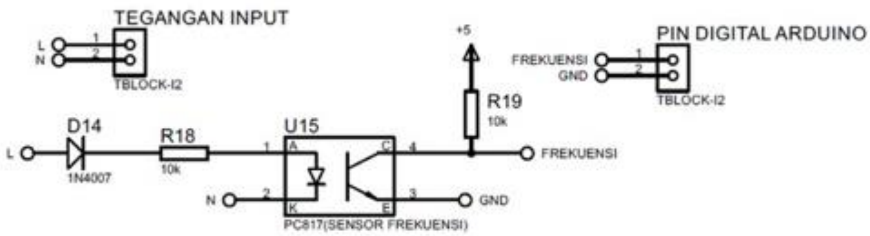

Figure 6. Schematic Diagram of the Frequency Sensor Circuit

3.1.4 Voltage and Current Sensors

Voltage and current sensors were arranged according to the quantities being measured at the SEIG output. The current sensor was connected in series with each conductor path, whereas the voltage sensor was connected in parallel with the relevant phase. This arrangement allows the controller to

P-ISSN: 1411-3414
E-ISSN: 2549-9815

acquire the electrical variables required for load regulation while limiting direct interaction between the measurement and power circuits.

Both sensors produce analog signals that are converted by the Arduino Mega's analog-to-digital converter and processed as real-time voltage and current measurements. These values form part of the feedback used by the ELC control routine.

A ZMPT101B single-phase AC sensor was selected for voltage measurement and an ACS712 sensor was used for current measurement (Figure 7 and Figure 8). Their voltage-level compatibility and straightforward interface with the Arduino platform support implementation of the proposed measurement circuit; measurement accuracy must be confirmed through calibration during prototype testing.

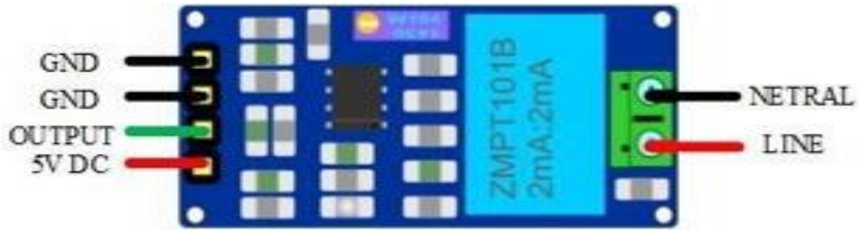

Figure 7. ZMPT101B Sensor

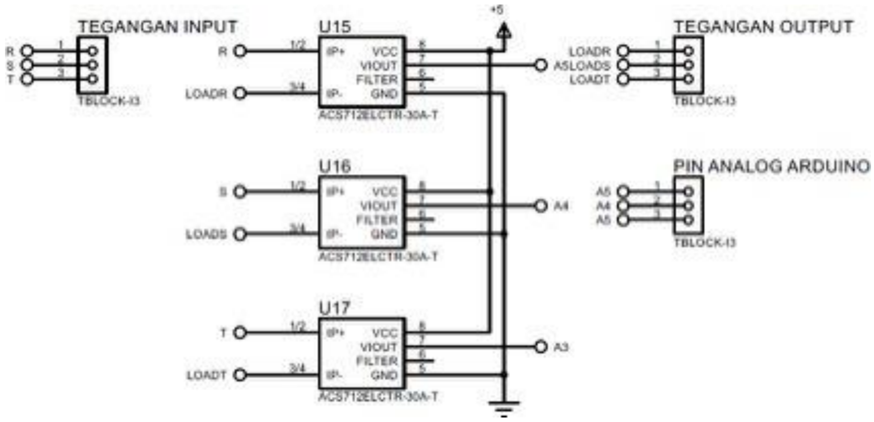

Figure 8. ACS712 Sensor

3.1.5 Gate Driver Design

The gate-driver circuit transfers switching commands from the microcontroller to the power semiconductors while maintaining electrical separation between the control and power stages (Figure 9). It therefore allows low-voltage logic signals to operate the TRIACs connected to the high-voltage AC circuit.

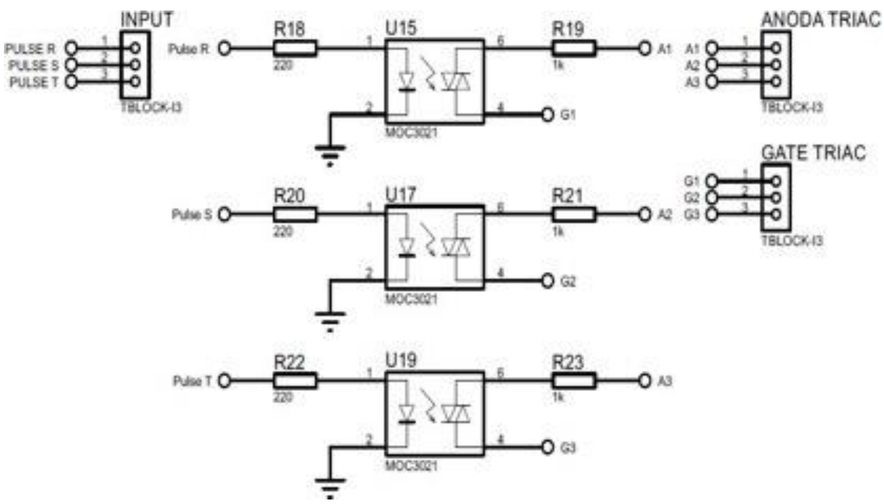

Figure 9. Schematic Diagram of the Gate Driver Circuit

P-ISSN: 1411-3414
E-ISSN: 2549-9815

The power stage uses a three-phase AC-AC converter to vary the voltage applied to the resistive dump load through phase-angle control (Figure 10). Direct AC regulation permits the absorbed power to be adjusted without changing the source frequency or introducing a DC-link conversion stage.

Each phase uses an independently triggered BTA12-600B TRIAC. The SEIG output is applied to the three power channels, and the control circuit determines the TRIAC firing angle for each phase. Changing the firing angle changes the RMS voltage and the power delivered to the corresponding dump-load branch. The arrangement is intended to absorb surplus active power and keep the generator loading closer to the required operating condition as consumer demand varies.

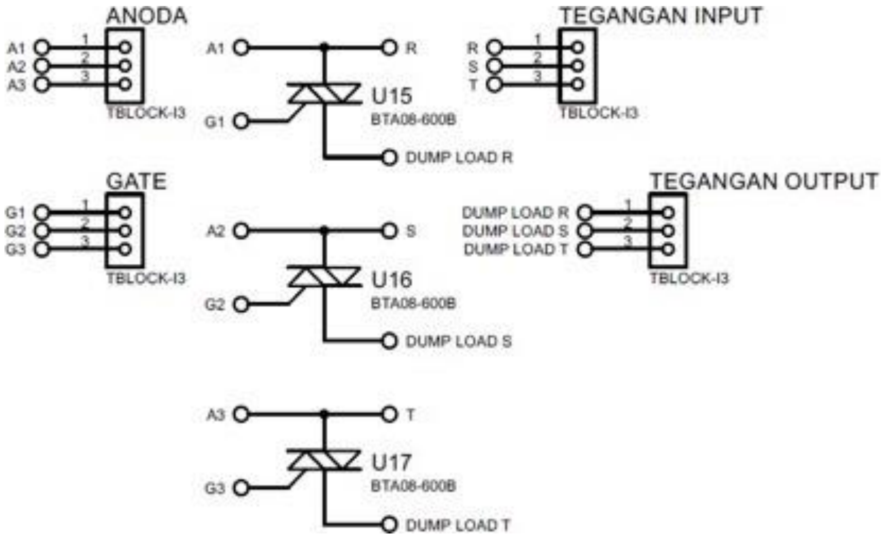

Figure 10. Schematic Diagram of the Power Circuit

Based on the design results, each subsystem performs a specific engineering function. The voltage and current sensors provide measurement signals to the microcontroller, while the zero-crossing detector and frequency sensor supply timing and frequency information. Meanwhile, the gate driver and TRIAC enable independent regulation of the dump-load power in each phase. This configuration indicates that the proposed hardware architecture incorporates the essential components required to implement three-phase load control.

However, the availability and integration of these components alone do not provide sufficient evidence that the system can maintain voltage and frequency stability or improve power quality. Verification of these performance objectives requires experimental testing using an induction generator under various operating conditions, including no-load operation, balanced and unbalanced loads, sudden load shedding, and gradual load addition. The parameters to be evaluated should include the RMS voltage of each phase, frequency deviation, phase currents, power diverted to the dump load, response time, overshoot, settling time, voltage unbalance, voltage and current total harmonic distortion, overall system efficiency, and the operating temperatures of the TRIACs and dump loads.

Therefore, the findings reported in this study are limited to demonstrating the feasibility of the proposed architecture and the successful integration of its hardware components. Validation of the control performance and power-quality characteristics will be conducted in the next stage, following the implementation of the control algorithm and experimental testing of the prototype under controlled operating conditions.

3.2 Discussion

Within the scope of a design study, the proposed ELC architecture addresses the main hardware functions required to support an induction-generator-based pico-hydropower plant: excitation, electrical measurement, isolated gate control, and controllable diversion of surplus active power. Its contribution lies in integrating these functions into a circuit arrangement that can be fabricated and tested, rather than in demonstrating regulation performance experimentally.

Stand-alone induction generation depends on the interaction among active-power demand, reactive-power support, and rotor speed. When consumer demand changes or differs among phases, the

P-ISSN: 1411-3414
E-ISSN: 2549-9815

electrical operating point may shift, and the output voltage and frequency may deviate from their intended values. By providing a controllable dump-load path, the ELC is intended to keep the total load presented to the generator closer to the required operating condition.

The three-phase AC-AC topology supports this objective with fewer conversion stages than an AC-DC-AC structure. Phase-angle control of the power switches changes the power delivered to the dump load while leaving the source frequency unchanged. The proposed arrangement can therefore compensate for changes in consumer demand at the power-distribution level; whether it provides acceptable voltage and frequency regulation must still be established experimentally.

The excitation-capacitor calculation is tied to the tested machine rather than selected solely from its nominal power. Nameplate data define the rated operating conditions, while the saturation test describes the relationship among generated voltage, magnetizing current, and rotational speed. Using the magnetizing reactance at 50 Hz as the calculation basis links the selected capacitance to the observed magnetization behavior of the 2.2 kW machine. Experimental self-excitation and voltage-regulation tests are still required to confirm the calculated value.

Electrical isolation is a consistent feature of the measurement and switching interfaces. Optoisolators in the zero-crossing detector, frequency sensor, and gate-driver circuits separate the Arduino-based control stage from the generator and converter voltages. This arrangement improves electrical safety and reduces the likelihood that switching transients will enter the low-voltage controller, although immunity to noise and surge conditions must be verified on the assembled prototype.

The ZMPT101B and ACS712 sensors provide an accessible feedback architecture for the Arduino Mega controller. Their integration allows voltage and current to be sampled alongside frequency, giving the controller the variables required to determine the generator's operating condition. Compatibility with the microcontroller, however, does not by itself establish measurement quality; calibration error, bandwidth, noise, and repeatability should be quantified during experimental testing.

Using one MOC3021 driver and one BTA12-600B TRIAC for each phase gives the controller three independent switching channels. This feature is relevant to unbalanced loading because the power directed to the dump load can be adjusted by phase rather than through a single common command. The effect of phase-angle control on waveform distortion, device heating, and interaction among the phases remains outside the evidence provided by the present design study.

Earlier ELC studies for isolated hydro generation have used AC-DC-AC conversion to regulate voltage and frequency [8], [9]. Such structures can provide broad control capability but require rectification and inversion stages. The present design instead uses direct AC-AC conversion, reducing the number of conversion stages and potentially simplifying fabrication and maintenance [9], [14]. This comparison concerns circuit architecture; the current study does not provide experimental evidence of lower cost or superior performance.

Previous research on Self-Excited Induction Generators has emphasized that excitation-capacitor selection directly affects voltage build-up and steady operation [14], [15]. The present design follows that principle by calculating capacitance from the motor nameplate and the measured saturation characteristic rather than from a generic rating alone. This approach relates the calculation to the actual machine data available in the study [7], [8], [16], although the resulting excitation performance still requires experimental confirmation.

Studies that concentrate on ELC control algorithms also indicate that controller performance depends on the quality of measurement signals and on the interfaces between the power stage and the control unit [17], [18]. The present article therefore gives specific attention to the zero-crossing detector, frequency sensor, voltage and current sensors, and optically isolated gate drivers. This emphasis defines the hardware foundation needed before any control algorithm can be evaluated reliably.

Unbalanced loading receives limited explicit treatment in the studies cited for comparison [19]-[23]. The proposed circuit assigns a separate TRIAC channel to phases R, S, and T, allowing per-phase adjustment rather than only aggregate power control. This architecture is conceptually suited to uneven three-phase consumer loads, although its advantage over globally controlled ELCs has not yet been tested [19]-[23].

Taken together, the novelty of the study lies in hardware integration rather than in a newly validated control algorithm. The direct three-phase AC-AC stage, machine-based excitation-capacitor calculation, isolated measurements, and independent gate channels are brought together as one ELC

P-ISSN: 1411-3414
E-ISSN: 2549-9815

design for an induction-generator-based pico-hydropower application. This combination addresses the need for a documented hardware platform that can proceed to fabrication and controlled testing.

The proposed design should therefore be interpreted as a technical basis for prototype development. Its direct conversion stage and per-phase channels may simplify implementation and offer flexibility under unequal loading, but reliability, regulation quality, harmonics, thermal performance, and long-term operation cannot be established from circuit design alone. These issues define the principal validation tasks for the next stage of the work.

4. Conclusion

This study developed the hardware design of a three-phase AC-AC converter-based Electronic Load Controller for a pico-hydropower system using a Self-Excited Induction Generator. The design integrates the excitation capacitor, voltage, current, and frequency measurement circuits, an Arduino Mega controller, isolated gate drivers, independently controlled TRIAC channels, and a resistive dump load. The architecture allows the power sent to the dump load to be adjusted without an intentional change to the source frequency and provides separate control of the three phases. These features make the design suitable for subsequent evaluation under balanced, varying, and unbalanced loads. The study did not include experimental prototype testing or quantitative assessment of voltage regulation, frequency stability, harmonics, thermal behavior, or long-term reliability. Future work should therefore fabricate and calibrate the prototype, define and evaluate the control algorithm, test balanced and unbalanced loading scenarios, and assess power quality, efficiency, device temperature, and sustained operation before practical performance claims are made.

References

[1] L. C. Alvear Pérez, M. J. Anaya Acosta, and C. A. Pedraza Yepes, "CFD simulation data of a pico-hydro turbine," Data Brief, vol. 33, p. 106596, Dec. 2020, doi: 10.1016/J.DIB.2020.106596.

[2] A. A. Lahimer, M. A. Alghoul, K. Sopian, N. Amin, N. Asim, and M. I. Fadhel, "Research and development aspects of pico-hydro power," Renewable and Sustainable Energy Reviews, vol. 16, no. 8, pp. 5861–5878, Oct. 2012, doi: 10.1016/J.RSER.2012.05.001.

[3] D. Powell, A. Ebrahimi, S. Nourbakhsh, M. Meshkahaldini, and A. M. Bilton, "Design of pico-hydro turbine generator systems for self-powered electrochemical water disinfection devices," Renew Energy, vol. 123, pp. 590–602, Aug. 2018, doi: 10.1016/J.RENENE.2017.12.079.

[4] K. Gaiser, P. Erickson, P. Stroeve, and J. P. Delplanque, "An experimental investigation of design parameters for pico-hydro Turgo turbines using a response surface methodology," Renew Energy, vol. 85, pp. 406–418, Jan. 2016, doi: 10.1016/J.RENENE.2015.06.049.

[5] M. F. Khan, M. R. Khan, and A. Iqbal, "Effects of induction machine parameters on its performance as a standalone self excited induction generator," Energy Reports, vol. 8, pp. 2302–2313, Nov. 2022, doi: 10.1016/J.EGYR.2022.01.023.

[6] V. B. M. Krishna, V. Sandeep, S. S. Murthy, and K. Yadlapati, "Experimental investigation on performance comparison of self excited induction generator and permanent magnet synchronous generator for small scale renewable energy applications," Renew Energy, vol. 195, pp. 431–441, Aug. 2022, doi: 10.1016/J.RENENE.2022.06.051.

[7] S. Sundaramoorthy and R. Essaki Raj, "Application of generalized hopfield neural network for the steady state analysis of self-excited induction generators," Appl Soft Comput, vol. 151, p. 111145, Jan. 2024, doi: 10.1016/J.ASOC.2023.111145.

[8] B. N. Roodsari, E. P. Nowicki, and P. Freere, "The Distributed Electronic Load Controller: A New Concept for Voltage Regulation in Microhydro Systems with Transfer of Excess Power to Households," Energy Procedia, vol. 57, pp. 1465–1474, Jan. 2014, doi: 10.1016/J.EGYPRO.2014.10.138.

[9] R. A. Ofosu, K. K. Kaberere, J. N. Nderu, and S. I. Kamau, "Design of BFA-optimized fuzzy electronic load controller for micro hydro power plants," Energy for Sustainable Development,

P-ISSN: 1411-3414
E-ISSN: 2549-9815

vol. 51, pp. 13–20, Aug. 2019, doi: 10.1016/J.ESD.2019.04.003.

[10] A. Ali, Arshad, H. Akhtar, M. U. R. Siddiqi, and M. Kamran, "An efficient and novel technique for electronic load controller to compensate the current and voltage harmonics," Engineering Science and Technology, an International Journal, vol. 23, no. 5, pp. 1042–1057, Oct. 2020, doi: 10.1016/J.JESTCH.2019.11.009.

[11] R. R. Singh, B. A. Kumar, D. Shruthi, R. Panda, and C. T. Raj, "Review and experimental illustrations of electronic load controller used in standalone Micro-Hydro generating plants," Engineering Science and Technology, an International Journal, vol. 21, no. 5, pp. 886–900, Oct. 2018, doi: 10.1016/J.JESTCH.2018.07.006.

[12] C. Xu, C. Xu, B. Li, S. Li, and T. Li, "Load-aware dynamic controller placement based on deep reinforcement learning in SDN-enabled mobile cloud-edge computing networks," Computer Networks, vol. 234, p. 109900, Oct. 2023, doi: 10.1016/J.COMNET.2023.109900.

[13] J. Titus and B. Ayalur, "Design and Fabrication of In-line Turbine for Pico Hydro Energy Recovery in Treated Sewage Water Distribution Line," Energy Procedia, vol. 156, pp. 133–138, Jan. 2019, doi: 10.1016/J.EGYPRO.2018.11.117.

[14] B. N. Nia Roodsari, E. P. Nowicki, and P. Freere, "A New Electronic Load Controller for the Self-excited Induction Generator to Decrease Stator Winding Stress," Energy Procedia, vol. 57, pp. 1455–1464, Jan. 2014, doi: 10.1016/J.EGYPRO.2014.10.137.

[15] S. C. Ndukwe, R. Kannan, and H. T. Wei, "Design and experimentation of a simple fuzzy pi-based ac chopper electronic load controller for pico hydropower system," Heliyon, vol. 10, no. 17, p. e35248, Sep. 2024, doi: 10.1016/J.HELIYON.2024.E35248.

[16] J. Samanta, S. Chakraborty, R. Sangno, and R. Pudur, "Study of power quality issues in a renewable-driven self-excited induction generator due to different loads at edge-off grid system," e-Prime - Advances in Electrical Engineering, Electronics and Energy, vol. 11, p. 100885, Mar. 2025, doi: 10.1016/J.PRIME.2024.100885.

[17] S. Chakraborty, J. Samanta, and R. Pudur, "Experimental analysis of a modified scheme for supplying single-phase remote loads from micro-hydro based three-phase self-excited induction generator," Measurement: Sensors, vol. 33, p. 101166, Jun. 2024, doi: 10.1016/J.MEASEN.2024.101166.

[18] L. K. Chanu, S. Chakraborty, and R. Pudur, "Real-time analysis of voltage and frequency regulation of self-excited induction generator based micro hydro plant using generalized impedance controller," Measurement: Sensors, vol. 33, p. 101235, Jun. 2024, doi: 10.1016/J.MEASEN.2024.101235.

[19] M. S. bin Abdul Rahim et al., "Experimental investigation on improving photovoltaic module efficiency using adaptive fuzzy-PID water cooling," Solar Energy, vol. 300, p. 113828, Nov. 2025, doi: 10.1016/J.SOLENER.2025.113828.

[20] M. F. A. Limon et al., "Grey wolf optimization-based fuzzy-PID controller for load frequency control in multi-area power systems," Journal of Automation and Intelligence, vol. 4, no. 2, pp. 145–159, Jun. 2025, doi: 10.1016/J.JAI.2025.01.002.

[21] E. R. J. Chullai, H. Nannam, P. Roy, R. Roy, and A. Banerjee, "Control and dynamic analysis of a BLDC-based pico-pump hydro energy storage system in a utility-interactive wind-based AC/DC microgrid," J Energy Storage, vol. 123, p. 116773, Jul. 2025, doi: 10.1016/J.EST.2025.116773.

[22] T. Ch. Singh, K. Srinivas Rao, P. Srinath Rajesh, and G. R. K. D. Satya Prasad, "Waste water-based pico-hydro power for automatic street light control through IOT-based sensors in smart cities: A pecuniary assessment," Artificial Intelligence and Machine Learning in Smart City Planning, pp. 87–99, Jan. 2023, doi: 10.1016/B978-0-323-99503-0.00010-7.

[23] A. Kadier et al., "A novel pico-hydro power (PHP)-Microbial electrolysis cell (MEC) coupled

P-ISSN: 1411-3414
E-ISSN: 2549-9815

system for sustainable hydrogen production during palm oil mill effluent (POME) wastewater treatment," Int J Hydrogen Energy, vol. 48, no. 55, pp. 21066–21087, Jun. 2023, doi: 10.1016/J.IJHYDENE.2022.09.023.